Chemical Physics xxx (2010) xxx–xxx

Contents lists available at ScienceDirect

Chemical Physics

journal homepage: www.elsevier.com/locate/chemphys

An initial value representation for the coherent state propagator with complex trajectories

Marcus A.M. de Aguiar *, Silvio A. Vitiello, Adriano Grigolo

Instituto de Física Gleb Wataghin, Universidade Estadual de Campinas, UNICAMP, 13083-970 Campinas, São Paulo, Brazil

ARTICLE INFO

Article history:
Received 12 August 2009
In final form 26 January 2010
Available online xxxx

Keywords:
Semiclassical methods
Coherent states
Initial value representations
Complex trajectories

ABSTRACT

We present an initial value representation for the semiclassical coherent state propagator based on complex trajectories. We map the complex phase space into a real one with twice as many dimensions and introduce initial valued trajectories in this *double phase space*. We use a procedure to eliminate non-contributing trajectories that allows for the automation of the entire calculation, rendering it simple. The resulting semiclassical formulas do not show divergences due to caustics and provide accurate results in short computational times.

1. Introduction

The investigation of wavepackets dynamics by semiclassical methods has practical importance for calculations of several processes involving atoms and molecules. It is also a fundamental topic in the study of the classical-quantum connection, especially for chaotic systems and for open systems, coupled to environments.

The history of semiclassical methods goes back to the origins of quantum mechanics itself. One fundamental result is the so called Van Vleck approximation to the coordinate propagator, derived in 1928 [1], that can be written as

$$\langle x_f|e^{-\widehat{iHT/\hbar}}|x_i\rangle \approx \frac{1}{\sqrt{2\pi i m_{qp}}} e^{\frac{i}{\hbar}S(x_i,x_f,T)-ik\frac{\pi}{2}}. \quad (1)$$

In this expression $S(x_i, x_f, T)$ is the classical action of a trajectory connecting coordinates x_i to x_f in the time T, m_{qp} is an element of the tangent matrix, that controls the motion in the vicinity of this trajectory, and k is the number of focal points (where m_{qp} goes to zero) along the trajectory. If more than one trajectory satisfying these boundary conditions exists, one has to sum their contributions. From this basic propagator one can compute the time evolution of arbitrary wavefunctions.

A more direct approach to calculate the time evolution of wavepackets is given by the propagator in the coherent state representation. The coherent states of the harmonic oscillator are minimum uncertainty wavepackets and define a representation involving both the coordinates and the momenta that can be readily visualized in the phase space. The coherent state propagator $\langle z_f|e^{-\frac{i}{\hbar}\widehat{HT}}|z_0\rangle$ represents the amplitude probability that the initial wavepacket $|z_0\rangle$ centered on q_0, p_0 is found at the state $|z_f\rangle$, centered on q_f, p_f, after a time T. The direct evaluation of the semiclassical limit of this propagator results in an expression bearing the same difficulties of the Van Vleck formula [2–5], namely: (a) the classical trajectories needed are defined by mixed initial-final boundary conditions, rendering the calculation hard, specially in multidimensional or chaotic systems; and (b) the formula diverges at phase space focal points. Moreover, the trajectories are complex and some of them, even satisfying the appropriate boundary conditions, lead to unphysical contributions and must be discarded [6–11,13,14].

Several methods have been developed to overcome these difficulties, most of them based on the idea of initial value representations (IVR) [15–24]. Among these, the Herman–Kluk propagator [18] and the method of linearized cellular dynamics developed by Heller and Tomsovic [25,26] stand out as very accurate. More recent derivations and corrections to the basic Herman–Kluk formula have also provided new insight into this class of approximations [27–30].

We should note that the coherent state representation is not the only way to do quantum mechanics in phase space. An important alternative is provided by the Wigner–Weyl representation of density operators [31–35]. A number of recent developments have demonstrated the viability of semiclassical methods applied to Wigner functions as a practical and efficient tool for propagation of molecular systems [36–38]. We shall not pursue this approach here and we refer to the article by Dittrich et al. [38] for a recent review.

* Corresponding author. Tel.: +55 19 3521 5466; fax: +55 19 3521 4146.
E-mail address: aguiar@ifi.unicamp.br (M.A.M. de Aguiar).

0301-0104/$ - see front matter © 2010 Elsevier B.V. All rights reserved.
doi:10.1016/j.chemphys.2010.01.020

In spite of the many difficulties involved in the calculation of the coherent state propagator with complex trajectories, this approximation turns out to be very accurate [8–10,12,13,39,40]. In this paper, we propose the construction of an initial value representation for this approximation that removes most of its problems: the complex trajectories are mapped into real trajectories of an associated Hamiltonian; the mixed conditions defining the trajectories are replaced by initial conditions; the divergences due to focal points are eliminated; and a simple and automatic filtering is used to eliminate the non-contributing trajectories.

The paper is organized as follows: Section 2 reviews the semiclassical coherent state propagator and its semiclassical approximation in terms of complex trajectories. In Section 3, we develop the initial value representation for complex trajectories (CIVR). It presents what we call the local CIVR, where only trajectories satisfying the original mixed conditions are considered, and the smooth CIVR where the neighborhood of the relevant trajectories is considered as well. We also discuss how the complex trajectories calculations are performed in terms of real trajectories. This section ends with a discussion of the criteria used for filtering out the non-contributing trajectories. In Section 4, the smooth CIVR is applied both to a 1D harmonic oscillator with a quartic perturbation and to a pure quartic oscillator. Because this work is a first step in the development of the CIVR, the numerical application is focused on the comparison between the present and previous approaches based on the direct computation of complex trajectories by root search techniques. Further comparisons with other methods such as the Herman–Kluk propagator and involving more difficult situations, such as chaos and multidimensional systems, will be considered in a separate paper. Section 5 is devoted to the conclusions and final comments. In two appendices useful properties of the tangent matrix are derived for both real and complex trajectories.

2. The semiclassical coherent state propagator

The coherent state $|z\rangle$ of a harmonic oscillator of mass m and frequency ω is defined by

$$|z\rangle = e^{-\frac{1}{2}|z|^2} e^{z\hat{a}^\dagger}|0\rangle \tag{2}$$

with $|0\rangle$ the harmonic oscillator ground state and

$$\hat{a}^\dagger = \frac{1}{\sqrt{2}}\left(\frac{\hat{q}}{b} - i\frac{\hat{p}}{c}\right), \quad z = \frac{1}{\sqrt{2}}\left(\frac{q}{b} + i\frac{p}{c}\right). \tag{3}$$

In these equations $\hat{q}$, $\hat{p}$, and $\hat{a}^\dagger$ are operators; q and p are real numbers and z is complex. The parameters $b = (\hbar/m\omega)^{\frac{1}{2}}$ and $c = (\hbar m\omega)^{\frac{1}{2}}$ define the length and momentum scales, respectively, and their product is $\hbar$.

For a time-independent Hamiltonian operator $\widehat{H}$, the propagator in the coherent state representation is the matrix element of the evolution operator between states $|z_0\rangle$ and $|z_f\rangle$ [41]:

$$K\left(z_f^*, z_0, T\right) = \langle z_f|e^{-\frac{i}{\hbar}\widehat{H}T}|z_0\rangle. \tag{4}$$

The semiclassical evaluation of $K\left(z_f^*, z_0, T\right)$ was presented in detail in [3,4]. The result is given by

$$K_{sc}\left(z_f^*, z_0, T\right) = \sum_v \sqrt{\frac{i}{\hbar}\frac{\partial^2 S}{\partial z_0 \partial z_f^*}} \exp\left\{\frac{i}{\hbar}(S+I) - \frac{1}{2}(|z_f|^2 + |z_0|^2)\right\}, \tag{5}$$

where

$$\begin{aligned} S &= S\left(z_f^*, z_0, T\right) \\ &= \int_0^T dt\left[\frac{i\hbar}{2}(\dot{u}v - \dot{v}u) - H(u,v,t)\right] - \frac{i\hbar}{2}\left(u(T)z_f^* + z_0 v(0)\right) \end{aligned} \tag{6}$$

is the action and the classical Hamiltonian function is calculated from the Hamiltonian operator as $H(u,v) = \langle v|\widehat{H}|u\rangle$. The term

$$I = \frac{1}{2}\int_0^T \frac{\partial^2 H}{\partial u \partial v}\, dt \tag{7}$$

is a correction to the action. The sum over v represents the sum over all contributing (complex) classical trajectories satisfying Hamilton's equations with boundary conditions

$$\frac{1}{\sqrt{2}}\left(\frac{q(0)}{b} + i\frac{p(0)}{c}\right) = z_0, \quad \frac{1}{\sqrt{2}}\left(\frac{q(T)}{b} - i\frac{p(T)}{c}\right) = z_f^*. \tag{8}$$

In all these expressions the variables u and v are defined by

$$u = \frac{1}{\sqrt{2}}\left(\frac{q}{b} + i\frac{p}{c}\right), \quad v = \frac{1}{\sqrt{2}}\left(\frac{q}{b} - i\frac{p}{c}\right). \tag{9}$$

They are manifestly independent ($u \neq v^*$ since q and p are complex), and replace z and z^* to avoid confusion. In these variables the boundary conditions become

$$u(0) = z_0, \quad v(T) = z_f^*. \tag{10}$$

We note that the second derivative of the action with respect to its arguments, as appearing in the pre-factor of the semiclassical propagator, can be written in terms of the tangent matrix, that controls the classical motion in the vicinity of a given trajectory. In Appendix A, we derive several useful relations between the tangent matrix in u, v and q, p variables for complex and real trajectories, including the well known relation

$$\frac{i}{\hbar}\frac{\partial^2 S}{\partial z_0 \partial z_f^*} = \frac{1}{M_{vv}}. \tag{11}$$

3. A complex initial value representation

3.1. Basic idea

The first of the boundary conditions (10) specifying the complex trajectory can be rewritten explicitly as

$$\frac{q(0)}{b} + ib\frac{p(0)}{\hbar} = \frac{q_0}{b} + ib\frac{p_0}{\hbar}, \tag{12}$$

where q_0 and p_0 are real and define the initial coherent state $|z_0\rangle$. This condition is not sufficient to determine the trajectory, since $q(0)$ and $p(0)$ are complex. The missing condition is given by the second equation in (10) and refers to the final propagation time T.

In order to avoid dealing with mixed initial–final conditions, let us suppose we had a second equation of the form

$$\frac{q(0)}{b} - ib\frac{p(0)}{\hbar} = \frac{q_1}{b} - ib\frac{p_1}{\hbar}, \tag{13}$$

where q_1 and p_1 are real parameters. In this case we could solve Eqs. (12) and (13) for $q(0)$ and $p(0)$ and find

$$\begin{aligned} q(0) &= \frac{1}{2}\left[(q_0+q_1) + i\frac{b^2}{\hbar}(p_0-p_1)\right], \\ p(0) &= \frac{1}{2}\left[(p_0+p_1) + i\frac{\hbar}{b^2}(q_1-q_0)\right]. \end{aligned} \tag{14}$$

For q_0 and p_0 fixed, each q_1 and p_1 defines a trajectory with end points $q(T,q_1,p_1)$ and $p(T,q_1,p_1)$. We call

$$v_1(T) = \frac{1}{\sqrt{2}}\left(\frac{q(T,q_1,p_1)}{b} - ib\frac{p(T,q_1,p_1)}{\hbar}\right). \tag{15}$$

Let $\tilde{q}_1$ and $\tilde{p}_1$ be the values of q_1 and p_1 such that the second of Eq. (10) is satisfied, i.e., for which the initial conditions (14) lead to $v_1(T) = v(T) = z_f^*$, or explicitly,

$$\begin{aligned} &Re[q(T,q_1,p_1) - ib^2 p(T,q_1,p_1)/\hbar] = q_f, \\ &Im[q(T,q_1,p_1)\hbar/b^2 - ip(T,q_1,p_1)] = -p_f, \end{aligned} \tag{16}$$

where q_f and p_f define the final coherent state $|z_f\rangle$.

With these considerations we can rewrite the semiclassical propagator as

$$K_{ivr}\left(z_f^*, z_0, T\right) = \int dq_1\, dp_1 K_{sc}\left(z_f^*, z_0, T\right)\delta_a(q_1 - \tilde{q}_1)\delta_a(p_1 - \tilde{p}_1), \tag{17}$$

where K_{sc} is given by Eq. (5). The notation δ_a stands for normalized Gaussian functions of width a, that tend to Dirac delta functions in the limit $a \to 0$. This equation is exact for all values of a, since the propagator can be taken out of the integral, which is normalized to one. In the limit $a \to 0$ the argument z_f^* in K_{sc} can be replaced by $v_1(T)$ and the trajectories in $K_{sc}(v_1(T), z_0, T)$ can be calculated according to the initial conditions (14). Their contributions are filtered out by the delta functions, which select only the trajectories satisfying the proper boundary conditions (10).

For nonzero a, on the other hand, a lot of flexibility is gained by expanding $K_{sc}\left(z_f^*, z_0, T\right)$ around $z_f^* = v_1(T)$. This procedure turns Eq. (17) into a true IVR expression, where not only the 'correct' trajectories satisfying (10) contribute to the propagator, but also their neighboring solutions. In spite of the integration over the auxiliary variables q_1 and p_1, the calculation of K_{ivr} becomes simpler because the trajectories involved are all given by initial conditions. However, in this case, K_{ivr} is not identical to K_{sc} anymore, but should be a good approximation if a is small. We shall see that this is indeed the case. Moreover, we will show that, contrary to K_{sc}, K_{ivr} does not diverge at focal points where M_{vv} goes to zero.

The equivalent expression of the semiclassical propagation for an arbitrary initial state described by the wave-function $\psi(z_0^*, 0) = \langle z_0|\psi\rangle$ is

$$\psi_{ivr}\left(z_f^*, T\right) = \frac{1}{2\pi\hbar}\int K_{ivr}\left(z_f^*, z_0, T\right)\psi(z_0^*, 0)\, dq_0\, dp_0. \tag{18}$$

Before we end this subsection we define the scaled variables $\bar{q} = q/b$, $\bar{p} = pb/\hbar$ and the scaled Hamiltonian

$$\overline{H}(\bar{q}, \bar{p}) = \frac{1}{\hbar}H(b\bar{q}, \hbar\bar{p}/b). \tag{19}$$

It is easy to check that the semiclassical expressions in terms of $\bar{q}$, $\bar{p}$ and $\overline{H}$ become identical to the original expressions with b and $\hbar$ replaced by 1. From now on we shall use these scaled variables, which amounts to set $b = \hbar = 1$, but will omit the bar to make the notation simpler. The original variables will be recovered later in the examples.

3.2. The calculation of complex trajectories

For analytic Hamiltonian functions $H(q,p)$ it is possible to rewrite the equations of motion for the complex variables q and p in terms of real trajectories of an auxiliary Hamiltonian system with twice as many degrees of freedom, or as we call it, the double phase space. We define [42,43]

$$q = Q_1 + iP_2, \quad p = P_1 + iQ_2 \tag{20}$$

and

$$H(q,p) = H_1(Q_1, Q_2, P_1, P_2) + iH_2(Q_1, Q_2, P_1, P_2), \tag{21}$$

where H_1 and H_2 are real functions of the real variables Q_1, Q_2, P_1, P_2. By the Cauchy–Riemann conditions it is easy to show that Hamilton's equations for q and p are equivalent to

$$\dot{Q}_i = \frac{\partial H_1}{\partial P_i}, \quad \dot{P}_i = -\frac{\partial H_1}{\partial Q_i}, \quad i = 1, 2. \tag{22}$$

Because the complex Hamiltonian H is conserved, both H_1 and H_2 are constants of the motion. In fact it can be shown that H_1 and H_2 are linearly independent, so that one-dimensional systems remain integrable in the double phase space, although the trajectories are generally unbound. The separation of variables in (20) may look unusual because it mixes q's and p's. However, it is the proper combination to get the correct signs in Hamilton's equations and it does look natural when the form of Eq. (14) is considered.

For the case $|\psi(0)\rangle = |z_0\rangle$, the real trajectory starting from the center of the wavepacket plays an important role, and we shall use it as a reference. Therefore, the integration over q_1 and p_1 in the CIVR will be centered on q_0 and p_0 and only a limited region around this point is expected to significantly contribute to the propagation. In this way we write

$$q_1 = q_0 + \Delta q, \quad p_1 = p_0 + \Delta p \tag{23}$$

and the initial conditions (14) reduce to

$$\begin{aligned} &Q_1(0) = q_0 + \Delta q/2, \quad Q_2(0) = \Delta q/2, \\ &P_1(0) = p_0 + \Delta p/2, \quad P_2(0) = -\Delta p/2. \end{aligned} \tag{24}$$

In accordance with Eq. (20), $q(0) = q_0 + w$, $p(0) = p_0 + iw$ with $w = (\Delta q - i\Delta p)/2$, which is exactly the variable used in a search procedure developed in Ref. [9].

3.3. The connection between initial and final displacements

A useful relation can be obtained through the connection between initial and final displacements in the q_1, p_1 plane. Comparing Eq. (20) with (14) we see that

$$\begin{aligned} Q_1(0) &= \frac{1}{2}(q_0 + q_1), \\ Q_2(0) &= \frac{1}{2}(q_1 - q_0), \\ P_1(0) &= \frac{1}{2}(p_0 + p_1), \\ P_2(0) &= \frac{1}{2}(p_0 - p_1), \end{aligned} \tag{25}$$

which also leads to $q_1 = Q_1(0) + Q_2(0)$ and $p_1 = P_1(0) - P_2(0)$. It turns out to be convenient to extend this definition to

$$\begin{aligned} q_1(t) &= Q_1(t) + Q_2(t), \\ p_1(t) &= P_1(t) - P_2(t). \end{aligned} \tag{26}$$

Because of the filtering functions δ_a in Eq. (17) the relevant contributions to the integrals over q_1 and p_1 come from the vicinities of $\tilde{q}_1$ and $\tilde{p}_1$, that should also be close to q_0 and p_0. For the trajectory starting exactly at $\tilde{q}_1$ and $\tilde{p}_1$ it follows, as already mentioned, that $v_1(T) = z_f^*$:

$$[Q_1(T) + iP_2(T)] - i[P_1(T) + iQ_2(T)] = q_f - ip_f \tag{27}$$

or, according to (26), $q_1(T) = q_f$ and $p_1(T) = p_f$.

For neighboring trajectories we may expand the final values of $q_1(T)$ and $p_1(T)$ around q_f and p_f as:

$$q_1(T) \approx q_f + \frac{\partial q_1(T)}{\partial q_1}(q_1 - \tilde{q}_1) + \frac{\partial q_1(T)}{\partial p_1}(p_1 - \tilde{p}_1),$$

$$p_1(T) \approx p_f + \frac{\partial p_1(T)}{\partial q_1}(q_1 - \tilde{q}_1) + \frac{\partial p_1(T)}{\partial p_1}(p_1 - \tilde{p}_1)$$

or

$$\begin{pmatrix} q_1(T)-q_f \\ p_1(T)-p_f \end{pmatrix} = \begin{pmatrix} \frac{\partial q_1(T)}{\partial q_1} & \frac{\partial q_1(T)}{\partial p_1} \\ \frac{\partial p_1(T)}{\partial q_1} & \frac{\partial p_1(T)}{\partial p_1} \end{pmatrix} \begin{pmatrix} q_1-\tilde{q}_1 \\ p_1-\tilde{p}_1 \end{pmatrix} \equiv \Lambda \begin{pmatrix} q_1-\tilde{q}_1 \\ p_1-\tilde{p}_1 \end{pmatrix}. \tag{28}$$

It follows that

$$\delta(q_1-\tilde{q}_1)\delta(p_1-\tilde{p}_1) = |\det \Lambda|\delta(q_1(T)-q_f)\delta(p_1(T)-p_f). \tag{29}$$

In Appendix B, Eq. (B.6), we show that $\det \Lambda = |M_{vv}|^2$.

3.4. Local complex initial value representation

In the case of delta functions we can use Eq. (29) to write down the first of our formulas, that we term *local* CIVR. Since

$$\frac{1}{\sqrt{2}}(q_1(T)-ip_1(T)) = v_1(T) \tag{30}$$

and defining

$$\delta^2\left(v_1(T)-z_f^*\right) = 2\pi\delta(q_1(T)-q_f)\delta(p_1(T)-p_f), \tag{31}$$

we obtain

$$\psi\left(z_f^*,T\right) = \int |M_{vv}|^{3/2} e^{i(S+I)-\frac{1}{2}(|z_f|^2+|z_0|^2)-i\frac{\xi}{2}} \psi\left(z_0^*,0\right)\delta^2\left(v_1(T)-z_f^*\right) \times \frac{d^2z_0}{\pi}\frac{d^2v_1}{\pi}, \tag{32}$$

where ξ is the phase of M_{vv}. Each pair of phase space points $q_0,\ p_0$ and $q_1,\ p_1$ define a complex trajectory with initial conditions

$$\begin{aligned} q(0) &= \frac{1}{2}(q_0+q_1)+i\frac{1}{2}(p_0-p_1), \\ p(0) &= \frac{1}{2}(p_0+p_1)+i\frac{1}{2}(q_1-q_0), \end{aligned} \tag{33}$$

which is equivalent to a real trajectory in the double phase space with initial conditions (25). The contribution of these trajectories to the final result is filtered by the delta function. The integration measures are defined as usual as $d^2z_0/\pi = dq_0dp_0/2\pi$ and $d^2v_1/\pi = dq_1dp_1/2\pi$.

The arguments of S and I in (32), which were originally $\left(z_f^*,z_0,T\right)$, were replaced by $(v_1(T),z_0,T)$, so that both S and I are computed using the trajectories defined by (33). Also important is the fact that M_{vv} in the pre-factor has moved from the denominator to the nominator, so that divergences at caustics are replaced by non-contributing trajectories. This is a well known property of IVR's constructed in this way. In practical calculations the delta functions may be replaced by thin box-like functions of size $a\times a$ in phase space. Similarly, the phase space of $q_f,\ p_f$ may be discretized as cells of size $a\times a$, so that all trajectories with end point $v_1(T)$ inside a given cell contribute to its central point. In this paper, we do not present numerical results using this method.

3.5. Smooth complex initial value representation

If the delta functions in the CIVR are replaced by Gaussian functions a better behaved approximation is obtained. Following Filinov [44] and Makri [45], we replace the filtering integrals of trajectories according to

$$\begin{aligned} \int \delta^2(v_1-\tilde{v})\frac{d^2v_1}{\pi} &\to \int e^{-\frac{1}{2a^2}[(q_1-\tilde{q}_1)^2+(p_1-\tilde{p}_1)^2]}\frac{d^2v_1}{\pi a^2} \\ &\approx \int e^{-\frac{1}{2a^2|M_{vv}|^2}[(q_1(T)-q_f)^2+(p_1(T)-p_f)^2]}\frac{d^2v_1}{\pi a^2} \\ &= \int |M_{vv}|^2 e^{-\frac{|v(T)-z_f^*|^2}{\alpha^2}}\frac{d^2v_1}{\pi\alpha^2}, \end{aligned} \tag{34}$$

where we have used Eq. (28) in the second line and defined the rescaled width

$$\alpha = a|M_{vv}|. \tag{35}$$

The use of smooth filters seems appropriate to coherent state propagation. It implies that not only the trajectories satisfying the exact boundary conditions (10) are considered, but also their neighborhood as defined by the parameter a. In this case the action $S\left(z_f^*,z_0,T\right)$ in Eq. (17) cannot be simply replaced by $S(v_1(T),z_0,T)$, but has to be expanded around each initial value trajectory up to second order. The result is

$$\begin{aligned} S\left(z_f^*,z_0,T\right) &\approx S(v_1(T),z_0,T)+\frac{\partial S}{\partial v(T)}\left(z_f^*-v_1(T)\right) \\ &\quad +\frac{1}{2}\frac{\partial^2 S}{\partial v(T)^2}\left(z_f^*-v_1(T)\right)^2 \\ &\approx S(v_1(T),z_0,T)-iu_1(T)\left(z_f^*-v_1(T)\right) \\ &\quad -i\frac{M_{uv}}{2M_{vv}}\left(z_f^*-v_1(T)\right)^2, \end{aligned} \tag{36}$$

where once again we have resorted to expressions derived in Appendix B.

The *smooth* CIVR can then be obtained by using Eqs. (34) and (36) in (18):

$$\psi\left(z_f^*,T\right) = \int |M_{vv}|^{3/2}\exp\left\{\phi-\frac{\left|v(T)-z_f^*\right|^2}{\alpha^2}\right\}\psi(z_0^*,0)\frac{d^2z_0}{\pi}\frac{d^2v_1}{\pi\alpha^2}, \tag{37}$$

where

$$\phi = i(S+I)+u_1(T)\left(z_f^*-v_1(T)\right)+\frac{M_{uv}}{2M_{vv}}\left(z_f^*-v(T)\right)^2-\frac{|z_f|^2}{2} -\frac{|z_0|^2}{2}-i\frac{\xi}{2}. \tag{38}$$

If the initial state to be propagate is itself a coherent state, Eq. (17), the smooth CIVR simplifies to

$$K\left(z_f^*,z_0,T\right) = \int |M_{vv}|^{3/2}\exp\left\{\phi-\frac{\left|v(T)-z_f^*\right|^2}{\alpha^2}\right\}\frac{d^2v_1}{\pi\alpha^2}. \tag{39}$$

In this paper, we shall discuss an example of this simple case only. All the tangent matrix elements appearing in Eqs. (38) and (39) can be readily computed from the tangent matrix of the real trajectory in the double phase space. This procedure eliminates the need to work with complex trajectories and also the so called root search problem, involved in finding trajectories with mixed initial–final conditions.

3.6. Filtering out non-contributing trajectories and choosing the smoothing factor α

The semiclassical expressions developed in the previous sections improve on the original semiclassical propagator by replacing the complex mixed conditions trajectories by real initial value solutions of a related Hamiltonian problem. This procedure also removes automatically the divergence problems cause by caustics. However, a number of important issues must still be handled before the local or smooth CIVR can be implemented on a computer.

The first of these issues concern the so called *non-contributing trajectories*. It is well known that not all trajectories satisfying the boundary conditions (10) should be included in the semiclassical propagator. The trajectories for which the real part of the exponent

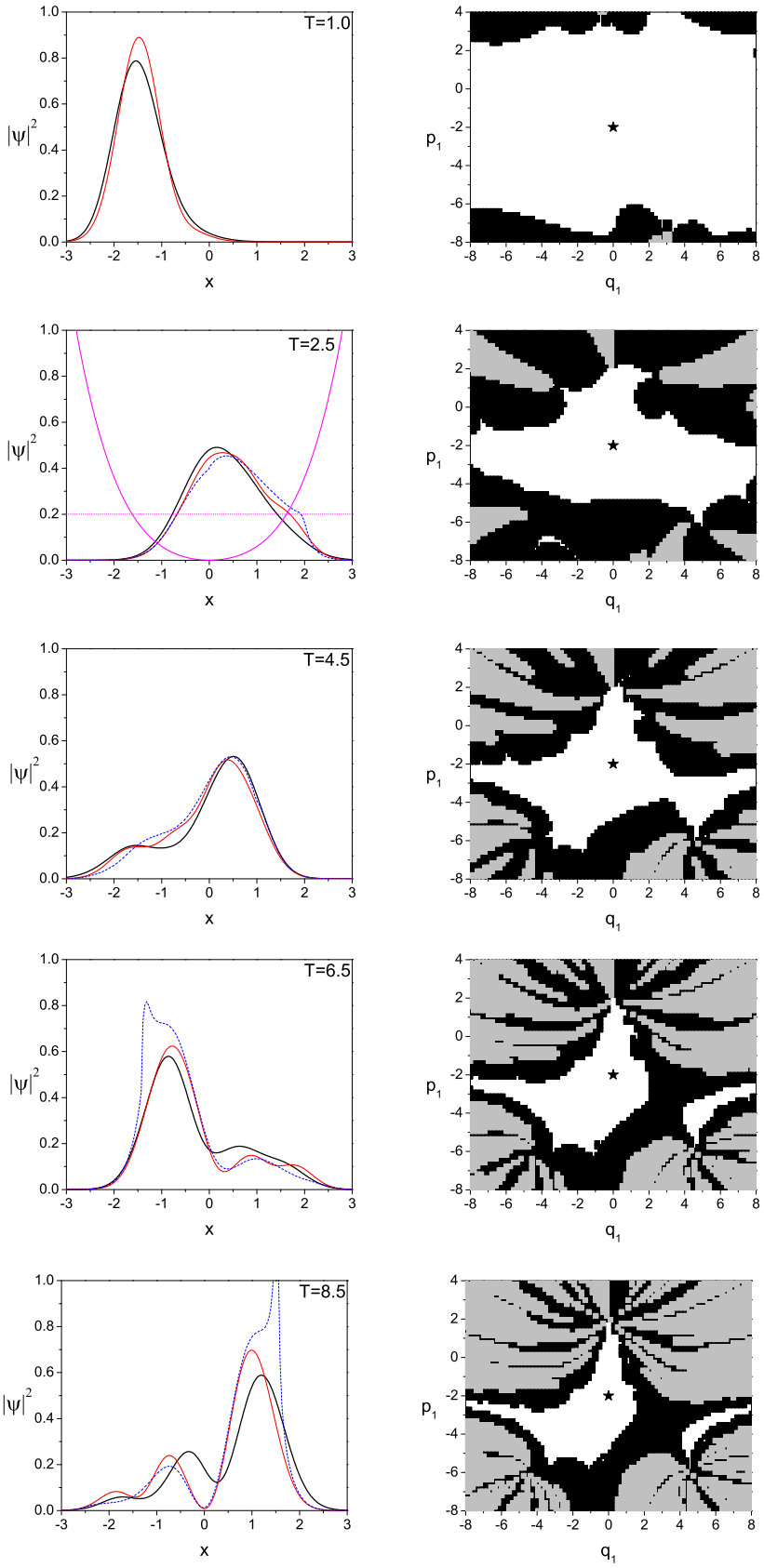

Fig. 1. The left panels show the exact and semiclassical square modulus of the wavefunctions for the given values of T. The thin continuous line (red) displays the exact result obtained via split time operator method; the thick solid (black) line is the CIVR approximation and the dashed line (blue) shows the result obtained in Ref. [14] by direct computation of contributing trajectories. For $T = 2.5$ we also show the potential $(V(x)/10)$ and the energy $E/10 = 0.2$ of the central trajectory (magenta). The right panels show the contributing and non-contributing initial trajectories in the q_1, p_1 plane as white and dark areas, respectively (see text). The star indicates the positions q_0 and p_0 of the initial wavepacket. (For interpretation of the references in color in this figure legend, the reader is referred to the web version of this article.)

Please cite this article in press as: M.A.M. de Aguiar et al., Chem. Phys. (2010), doi:10.1016/j.chemphys.2010.01.020

ϕ in (38) is positive must be discarded as they give rise to divergent contributions in the semiclassical limit. These trajectories are probably associated with forbidden deformations of the integration contours that appear in the derivation of the semiclassical approximation (4). For the harmonic oscillator it can be checked explicitly that Eqs. (38) and (39) give exact results and also that $Re(\phi) \leqslant 0$ for all complex trajectories. For finite $\hbar$, trajectories with $0 < Re(\phi) < \hbar$ can still be included without causing semiclassical divergences. In our calculations, we discard trajectories satisfying

$$Re(\phi) > \hbar. \tag{40}$$

Another usual numerical problem is related to the growth of the tangent matrix element M_{vv} for unstable trajectories. For the harmonic oscillator $|M_{vv}| = 1$ for all trajectories, but for general Hamiltonians $|M_{vv}|$ can become large giving rise to unphysical contributions. In order to avoid such situations we also discard trajectories satisfying

$$|M_{vv}| > d, \tag{41}$$

where d is going to be the only adjustable parameter of our calculations.

Finally, we have to choose the width of the Gaussian smoothing a. If a is too small we should recover the exact propagator K_{sc}, which is not necessarily a good strategy. In this limit the caustic problems return and the numerical calculation of the many trajectories for each value of q_1 and p_1 is wasted, since only those satisfying the boundary conditions (10) are retained. Many prescriptions for fixing a can be devised (see, for instance [44,45]) and the results vary accordingly. So far we do not have a theory for choosing the best width and we will limit ourselves here to a single possibility, namely

$$a = |M_{vv}|^{-1/2}. \tag{42}$$

This choice balances the range of influence of each trajectory according to their stability and seems to work uniformly well for all the cases tested. The re-scaled width becomes $\alpha = |M_{vv}|^{1/2}$ and the combination appearing in the pre-factor becomes $|M_{vv}|^{3/2}/\alpha^2 = |M_{vv}|^{1/2}$.

4. Example

As a simple application of the smooth CIVR we consider the system

$$\widehat{H} = \frac{1}{2}\hat{p}^2 + \frac{\Omega^2}{2}\hat{q}^2 + \frac{\lambda}{4}\hat{q}^4. \tag{43}$$

This problem was studied also in [14] for the parameters $\Omega = 1$, $\lambda = 0.4$ and $\hbar = 1$ by directly computing the relevant complex trajectories. For these values the ground state energy is

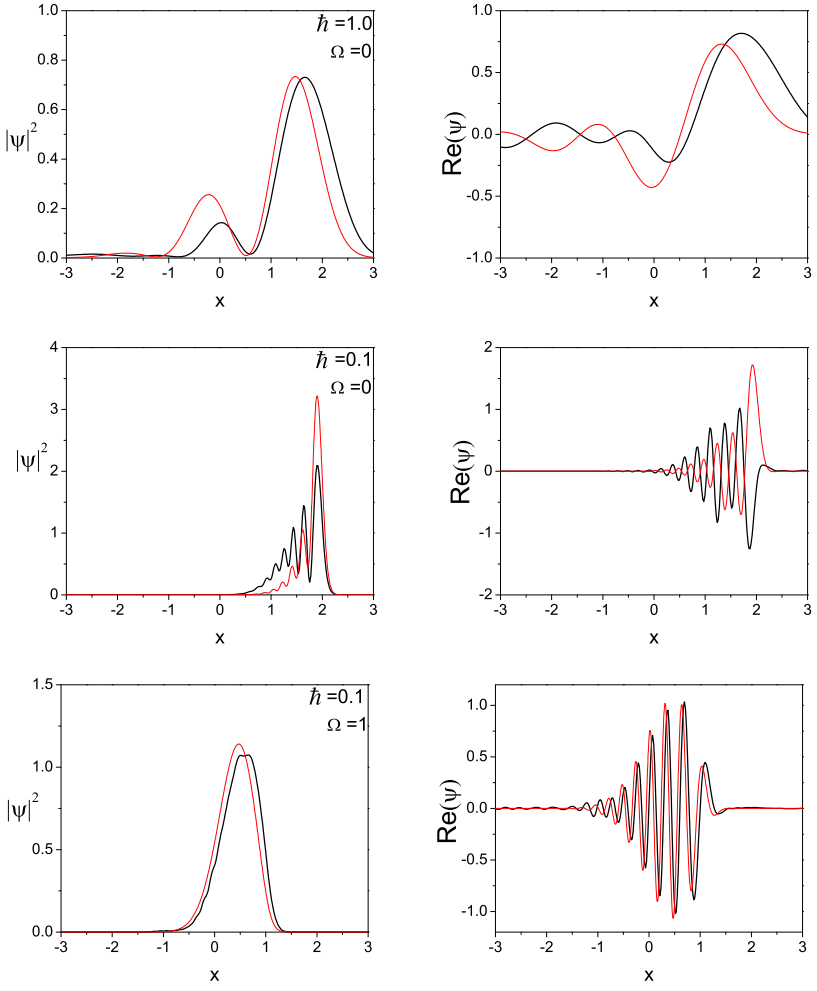

Fig. 2. Exact and semiclassical results for $T = 4.5$. The left panels show the square modulus of the wavefunctions and the right panels their real part. The thin continuous line (red) displays the exact result obtained via split time operator method; the thick solid line (black) is the CIVR approximation. From top to bottom the pairs of plots correspond to $\hbar = 1$, $\Omega = 0$; $\hbar = 0.1$, $\Omega = 0$; and $\hbar = 0.1$, $\Omega = 1$. (For interpretation of the references in color in this figure legend, the reader is referred to the web version of this article.)

$E_0 \approx 0.559$ and the first two excited states have $E_1 \approx 1.770$ and $E_2 \approx 3.319$. For the initial wavepacket we choose $q_0 = 0,\ p_0 = -2.0$, and $b = 1.0$. This gives $E = H(q,p) = 2.0$ for the energy of the central trajectory, $\tau \approx 4.7$ for its period, and $X_{\text{turn}} \approx \pm 1.6$ for its turning points. Fig. 1(T=2.5) shows a plot of the potential function and also indicates the energy of central trajectory.

We momentarily restore the original un-scaled variables to illustrate both the computation of the classical Hamiltonian and the scaling process. The classical Hamiltonian function is

$$H = \frac{1}{2}p^2 + \frac{1}{2}\left(\Omega^2 + \frac{3\lambda b^2}{4}\right)q^2 + \frac{\lambda}{4}q^4 + \left(\frac{\hbar^2}{4b^2} + \frac{\Omega^2 b^2}{4} + \frac{3\lambda b^4}{16}\right), \quad (44)$$

where b is the width of the wavepacket. In terms of scaled variables (see Eq. (19)) the Hamiltonian becomes

$$\overline{H} = \omega\left[\frac{1}{2}\bar{p}^2 + \frac{1}{2}\bar{\nu}^2 q^2 + \frac{\bar{\lambda}}{4}\bar{q}^4 + \frac{1}{4}\left(1 + \nu^2 + \frac{3\bar{\lambda}}{16}\right)\right], \quad (45)$$

where $\omega = \hbar/b^2,\ \nu = \Omega/\omega,\ \bar{\lambda} = \lambda\hbar/\omega^3$, and $\bar{\nu}^2 = \nu^2 + 3\bar{\lambda}/2$. For the values used in [14] and in Fig. 1, $\hbar = \Omega = b = 1$, we have $\omega = \nu = 1,\ \bar{\lambda} = 0.4$, and $\bar{\nu}^2 = 1.6$.

Fig. 1 shows five snapshots of the wavepacket (left column). The corresponding regions of the $q_1,\ p_1$ plane where trajectories contribute to the propagation are shown as white areas in the plots on the right column. The gray regions correspond to unbound trajectories, that tend to escape to infinity, and do not contribute significantly because $Re(\phi) \ll -\hbar$. The trajectories on the black regions have been eliminated because either $Re(\phi) > \hbar$ or $|M_{vv}| > d$ (see Eqs. (40) and (41)). In all these figures we have fixed the constant $d = 5.0$. The integration over q_1 and p_1 was performed using a regular grid with 80 points in q_1, centered on zero and varying from -8 to 8, and 60 points in p_1 centered on -2 and varying from -10 to 6. The computational time for the present semiclassical calculation is longer than the split-time operator method (STOM), well known for being efficient and accurate for one-dimensional problems. For $T = 8.5$ the calculations take about 8 s in a Core 2 Quad PC with 2.4 GHz, as opposed to about 4 s of the STOM. However, the computational time drops to 5 s if the ranges of integration are changed from -6 to 6 and from -4 to 4 in q_1 and p_1, respectively, without altering significantly the results.

The wavefunctions in Fig. 1 were calculated using the simple discretization

$$\psi(x,T) = \sum_{n,m}\langle x|z_{nm}\rangle K(z^*_{nm}, z_0, T)\,\frac{\Delta q \Delta p}{2\pi}, \quad (46)$$

where n and m represent the grid in phase space centered on the origin. We used a total of 40 and 60 points in the q and p directions, respectively, with $-4 < q_n < +4$ and $-6 < p_m < +6$.

Fig. 2 shows results for different sets of parameters. The left panels show the square modulus of the wavefunctions and the right panels their real part. The first two pairs of panels show calculations for a pure quartic oscillator, $\Omega = 0$, and the two values $\hbar = 1$ and $\hbar = 0.1$. The last pair shows results for $\hbar = 0.1$, $\Omega = 1$. For $\hbar = 0.1$ we used $d = 4$ and the relevant integration interval in q_1 and p_1 was reduced. The computational time dropped to about 2 s, which is faster than the STOM, which still takes about 3 s. The results are still very good, except maybe for $\hbar = 0.1,\ \Omega = 0$. In this case the wavepacket is close to the turning point, where the approximation is expected to be not so good. Indeed, we show in Fig. 3 the analogous results for $T = 5.3$, away from the turning point, where very good agreement is obtained again. An obvious problem with the case $\hbar = 0.1,\ \Omega = 0$ is the phase mismatch between exact and semiclassical results. The phase difference between the semiclassical and the exact solutions increases slowly for short times, but suffers faster changes at the turning points when the wavepacket oscillates faster, like close to $T = 4$.

5. Conclusions

In this paper, we have presented an initial value representation for the semiclassical coherent state propagator given in terms of complex classical trajectories. We mapped the complex trajectories of the original Hamiltonian system into real trajectories of a related Hamiltonian system with twice as many degrees of freedom, dubbed the *double phase space*. By introducing an extra integration over auxiliary phase space variables we also replaced the mixed conditions trajectories by initial value solutions in the double phase space. Simple criteria were also introduced to automatically remove non-contributing solutions.

The results obtained with this method are accurate and fast, even considering the extra integration that has been introduced. This is especially significant when compared to previous calculations using root search procedures [14]. Comparison with other methods, such as Herman–Kluk, are the obvious next step to establish the usefulness of the procedure. Work in this direction is under way.

In spite of the accuracy of our results, a few details remain to be understood with room for further improvements. One of the questions is how to chose the best width a or how to properly justify the choice $a = |M_{vv}|^{-1/2}$ made in the present calculations. In specific cases, different choices for a might give better results. In fact, in several cases the value of a can be adjusted to improve the semiclassical result. An interesting alternative is to use the procedure devised in [45], where the width is chosen to minimize the oscillations of the integrand. This shows that a better theoretical understanding on the role of a is needed. Another problem is that the propagated wavepackets turn out not to be properly normalized, and the amount by which normalization is lost also depends on a. In Figs. 1–3, the wavefunctions have been re-normalized by hand after the propagation.

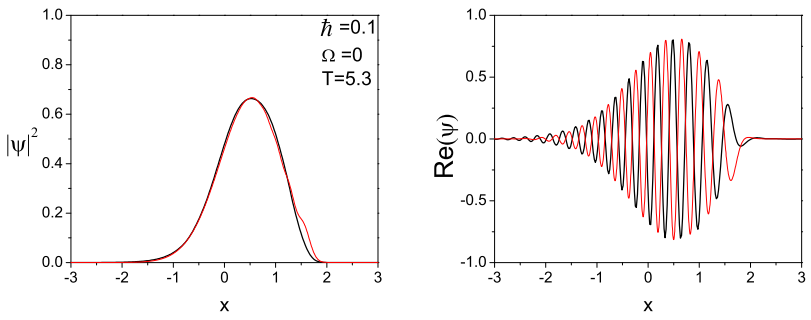

Fig. 3. Same as in Fig. 2 for $T = 5.3,\ \hbar = 0.1$ and $\Omega = 0$.

Despite these problems the method improves the results obtained by direct computation of the contributing trajectories and is much faster and simple to program. The next steps, besides comparison with other semiclassical methods, includes applications to multidimensional and chaotic systems, where the integrations over the initial conditions may be performed by Monte Carlo techniques.

Acknowledgements

Support from FAPESP and CNPq (Brazil) is acknowledged. Facilities of the CENAPAD high-performance computing center at Universidade Estadual de Campinas where used in this work.

Appendix A. Tangent matrices

In this appendix, we use the scaled units where $\hbar = b = 1$. In the u and v variables the tangent matrix is defined by

$$\begin{pmatrix} \delta u(T) \\ \delta v(T) \end{pmatrix} = \begin{pmatrix} M_{uu} & M_{uv} \\ M_{vu} & M_{vv} \end{pmatrix} \begin{pmatrix} \delta u(0) \\ \delta v(0) \end{pmatrix}, \tag{A.1}$$

where $\delta u(0)$ and $\delta v(0)$ are small displacements at the initial point of the trajectory and $\delta u(T)$ and $\delta v(T)$ are the corresponding final deviations. The action $S(v'', u', T)$ for the trajectory with $u(0) = u'$ and $v(T) = v''$ satisfies [3]

$$u(T) \equiv u'' = i\frac{\partial S}{\partial v''}, \quad v(0) \equiv v' = i\frac{\partial S}{\partial u'}. \tag{A.2}$$

From the differentiation of (A.2) keeping the variable T constant, we can obtain the connection between initial and final displacements. In matrix form it is

$$\begin{pmatrix} \delta u(T) \\ \delta v(0) \end{pmatrix} = i\begin{pmatrix} S_{uu} & S_{uv} \\ S_{vu} & S_{vv} \end{pmatrix} \begin{pmatrix} \delta u(0) \\ \delta v(T) \end{pmatrix}, \tag{A.3}$$

where $S_{uv} = \partial^2 S/\partial u' \partial v''$, etc. Comparing with Eq. (A.1) we find

$$S_{uv} = -iM_{vv}^{-1}, \quad S_{vv} = -i\frac{M_{uv}}{M_{vv}}. \tag{A.4}$$

Using the definition of u and v in terms of q and p (notice that all these variables are complex) it is easy to show that [3]

$$\begin{aligned} M_{uu} &= \frac{1}{2}(m_{qq} + m_{pp} + im_{pq} - im_{qp}), \\ M_{uv} &= \frac{1}{2}(m_{qq} - m_{pp} + im_{pq} + im_{qp}), \\ M_{vu} &= \frac{1}{2}(m_{qq} - m_{pp} - im_{pq} - im_{qp}), \\ M_{vv} &= \frac{1}{2}(m_{qq} + m_{pp} - im_{pq} + im_{qp}), \end{aligned} \tag{A.5}$$

where m is the tangent matrix in the q, p system. Finally, using the definition of the real variables $Q_1,\ Q_2,\ P_1,\ P_2$ and defining its corresponding 4×4 tangent matrix n we can show that

$$\begin{aligned} m_{qq} &= n_{11} - in_{14}, \\ m_{qp} &= n_{13} - in_{12}, \\ m_{pq} &= n_{24} + in_{21}, \\ m_{pp} &= n_{22} + in_{23}. \end{aligned} \tag{A.6}$$

Therefore, by working directly with the real trajectories in the double phase space we can compute n and reconstruct the matrices m and M using simple linear transformations.

Appendix B. Calculation of det Λ

If $v(T)$ in Eq. (30) is an analytic function of the initial condition v_1, then, by the Cauchy–Riemann conditions we have

$$\frac{\partial q_1(T)}{\partial q_1} = \frac{\partial p_1(T)}{\partial p_1}, \quad \frac{\partial q_1(T)}{\partial p_1} = -\frac{\partial p_1(T)}{\partial q_1}. \tag{B.1}$$

By the definition of Λ, Eq. (28),

$$\det \Lambda = \left(\frac{\partial q_1(T)}{\partial q_1}\right)^2 + \left(\frac{\partial q_1(T)}{\partial p_1}\right)^2. \tag{B.2}$$

On the other hand we also have,

$$\begin{aligned} \frac{\partial v(T)}{\partial v_1} &= \frac{1}{\sqrt{2}}\left(\frac{\partial}{\partial q_1} + i\frac{\partial}{\partial p_1}\right)\frac{1}{\sqrt{2}}(q_1(T) - ip_1(T)) \\ &= \frac{1}{2}\left(\frac{\partial q_1(T)}{\partial q_1} + \frac{\partial p_1(T)}{\partial p_1}\right) + \frac{i}{2}\left(\frac{\partial q_1(T)}{\partial p_1} - \frac{\partial p_1(T)}{\partial q_1}\right) \\ &= \frac{\partial q_1(T)}{\partial q_1} + i\frac{\partial q_1(T)}{\partial p_1} \end{aligned} \tag{B.3}$$

and, therefore,

$$\det \Lambda = \left|\frac{\partial v(T)}{\partial v_1}\right|^2. \tag{B.4}$$

Finally, using the second of Eq. (A.2) with $v' = v_1$, and differentiating with respect to $v(T)$,

$$\frac{\partial v_1}{\partial v(T)} = i\frac{\partial^2 S}{\partial u' \partial v(T)}, \tag{B.5}$$

which implies

$$\det \Lambda = \left|i\frac{\partial^2 S}{\partial u' \partial v(T)}\right|^{-2} = |M_{vv}|^2 \tag{B.6}$$

by Eq. (A.4).

References

[1] J.H. Van Vleck, Proc. Natl. Acad. Sci. 14 (1928) 178.
[2] J.R. Klauder, B.S. Skagerstam, Coherent States, Applications in Physics and Mathematical Physics, World Scientific, Singapore, 1985.
[3] M. Baranger, M.A.M. de Aguiar, F. Keck, H.J. Korsch, B. Schellhaaß, J. Phys. A 34 (2001) 7227.
[4] E. Martn-Fierro, J.M.G. Llorente, J. Phys. A 40 (2007) 1065.
[5] C. Braun, A.J. Garg, Math. Phys. 48 (2007) 32104.
[6] D. Huber, E.J. Heller, J. Chem. Phys. 87 (1987) 5302.
[7] D. Huber, E.J. Heller, R.G. Littlejohn, J. Chem. Phys. 89 (1988) 2003.
[8] S. Adachi, Ann. Phys. (NY) 195 (1989) 45.
[9] A. Rubin, J.R. Klauder, Ann. Phys. (NY) 241 (1995) 212.
[10] A. Shudo, K.S. Ikeda, Phys. Rev. Lett. 74 (1995) 682.
[11] A. Shudo, K.S. Ikeda, Phys. Rev. Lett. 76 (1996) 4151.
[12] T. Van Voorhis, E.J. Heller, Phys. Rev. A 66 (2002) 50501.
[13] A.D. Ribeiro, M.A.M. de Aguiar, M. Baranger, Phys. Rev. E 69 (2004) 066204.
[14] M.A.M. de Aguiar, M. Baranger, L. Jaubert, F. Parisio, A.D. Ribeiro, J. Phys. A 38 (2005) 4645.
[15] W.H. Miller, J. Chem. Phys. 53 (1970) 3578.
[16] W.H. Miller, Adv. Chem. Phys. 25 (1974) 69.
[17] E.J. Heller, J. Chem. Phys. 62 (4) (1975) 1544.
[18] M.F. Herman, E. Kluk, Chem. Phys. 91 (1984) 27.
[19] K.G. Kay, J. Chem. Phys. 100 (6) (1994) 4377.
[20] K.G. Kay, J. Chem. Phys. 100 (1994) 4432.
[21] K.G. Kay, J. Chem. Phys. 107 (1997) 2313.
[22] W.H. Miller, J. Phys. Chem. A 105 (2001) 2942.
[23] S. Zhang, E. Pollak, Phys. Rev. Lett. 91 (2003) 190201.
[24] D.H. Zhang, E. Pollak, Phys. Rev. Lett. 93 (2004) 140401.
[25] E.J. Heller, J. Chem. Phys. 94 (1991) 2723.
[26] S. Tomsovic, E. Heller, Phys. Rev. Lett. 67 (1991) 664.
[27] D.V. Shalashilin, M.S. Child, Chem. Phys. 304 (2004) 103.
[28] D.V. Shalashilin, I. Burghardt, J. Chem. Phys. 129 (2008) 084104.
[29] E. Pollak, J. Shao, J. Phys. Chem. A 107 (2003) 7112.
[30] K.G. Kay, Chem. Phys. 322 (2006) 3.
[31] E.P. Wigner, Phys. Rev. 40 (1932) 749.
[32] M. Hillery, R.F. O'Connel, M.O. Scully, E.P. Wigner, Phys. Rep. 106 (1984) 121.
[33] M.V. Berry, Proc. R. Soc. Lond. A423 (1989) 219.

Please cite this article in press as: M.A.M. de Aguiar et al., Chem. Phys. (2010), doi:10.1016/j.chemphys.2010.01.020

[34] M.S. Marinov, Phys. Lett. A153 (1991) 5.
[35] A.M. Ozorio de Almeida, Phys. Rep. 295 (1998) 265.
[36] T. Dittrich, C. Viviescas, L. Sandoval, Phys. Rev. Lett. 96 (2003) 070403.
[37] T. Dittrich, L.A. Pachon, Phys. Rev. Lett. 102 (2009) 150401.
[38] T. Dittrich, E.A. Gomez, L.A. Pachon, arXiv:0911.3871v1 (physics.chem-ph).
[39] Y. Goldfarb, I. Degani, D.J. Tannor, J. Chem. Phys. 125 (2006) 231103.
[40] Y. Goldfarb, D.J. Tannor, J. Chem. Phys. 127 (2007) 161101.
[41] J.R. Klauder, in: G. Papanicolau (Ed.), Random Media, The IMA Volume in Mathematics and Its Applications, vol. 7, Springer-Verlag, New York, 1987, p. 163.
[42] A.L. Xavier Jr., M.A.M. de Aguiar, Ann. Phys. (NY) 252 (1996) 458.
[43] R.S. Kaushal, H.J. Korsch, Phys. Lett. A276 (2000) 47.
[44] V.S. Filinov, Nucl. Phys. B271 (1986) 717.
[45] N. Makri, H. Miller, Chem. Phys. Lett. 139 (1987) 10.

Please cite this article in press as: M.A.M. de Aguiar et al., Chem. Phys. (2010), doi:10.1016/j.chemphys.2010.01.020